Numerical investigations of turbulent premixed flame ignition by a series of Nanosecond Repetitively Pulsed discharges

Yacine Bechane, Benoit Fiorina

Numerical investigations of turbulent premixed flame ignition by a series of Nanosecond Repetitively Pulsed discharges

Yacine Bechane[a,*], Benoît Fiorina[a]

[a]*Laboratoire EM2C, CNRS, CentraleSupélec, Université Paris-Saclay, 3, Joliot Curie,91192 Gif-sur-Yvette, France*

Abstract

Nanosecond Repetitively Pulsed (NRP) discharges are an efficient way to promote turbulent flame ignition in lean regimes. The energy released by NRP discharges leads first to an ultra-fast species dissociation and heating phenomena, followed by a slow heating process. A phenomenological plasma model is presented to capture the influence of NRP discharges on the combustion process at low CPU cost. The model is here implemented in a LES flow solver to simulate the ignition sequence of a bluff-body turbulent premixed flame by a series of NRP discharges. Two numerical computations are performed. First, only the thermal effects of the discharge (ultra-fast heating and slow heating due to vibrational energy relaxation) are taken into account. Then both the thermal and chemical effects (mainly O_2 dissociation into O) are considered. The results show that in the first simulation the ignition never occur, whereas in the second simulation flame ignition occurs after only 5 pulses. The ignition success or failure results from a competition

*Corresponding author:
Email address: yacine.bechane@centralesupelec.fr (Yacine Bechane)

between the residence time of the reacting gases in the discharge channel and the combustion chemistry time scale. A low-order model based on a perfectly stirred reactor (PSR) is then derived. It confirms that the atomic O produced during the discharge enhances the methane oxidation reactions, reducing the combustion chemistry time scale and leading to a successful ignition. PSR results are used to build-up a plasma-assisted ignition diagram which indicates the number of pulses required to form a turbulent flame kernel.
Keywords:
Plasma-assisted combustion, Nanosecond Repetitively Pulsed discharges, Turbulent premixed flame, Large Eddy Simulation

---

Colloquium: New concepts

Length of the paper determined using Method 2.
Total length of the paper: 7.5 pages

The authors will pay color reproduction charges if applicable.

1. Introduction

To reduce pollutant emissions such as nitrogen oxides, lean combustion chambers are under development in many energy-related sectors. However, a recurring problem to industrial applications is that lowering the flame temperature slows the chemical reactions, causing difficulties to ensure successful ignitions over the wide range of operating conditions covered by practical applications.

An emerging solution to promote ignition is to generate high-voltage electric discharges between two electrodes located inside the combustion

chamber. It generates locally a plasma, which interacts with the combustion. Beneficial effects of plasma-assisted combustion have been observed in laboratory-scale burners under the action of microwave discharges, gliding arc discharges, plasma torches, nanosecond dielectric barrier discharges or Nanosecond Repetitively Pulsed (NRP) discharges [1, 2]. Among these various types of discharges, Nanosecond Repetitively Pulsed (NRP) discharges [3, 4] have shown to be a particularly energy-efficient way to initiate and control combustion processes especially when conventional ignition systems such as spark plugs are rather ineffective or too energy costly [2].

Efficiency of NRP discharges is high because the energy of the electric discharge is not only spent to increase the gas temperature but also to generate active species [5]. In typical conditions, around 35% of molecular oxygen is dissociated in the inter-electrode region [5, 6]. This high concentration of radicals has a positive effect on ignition phenomena [7]. Experiments conducted in closed vessel showed that NRP discharges greatly improve ignition probability over different flow conditions [8] but also revealed the complexity of the ignition mechanism. For instance, a larger amount of energy deposition or higher pulse frequency do not necessarily lead to a higher ignition probability [9]. To fully control the ignition by NRP discharge a complete understanding of the governing physics and the impact of the different discharge parameters is necessary.

Numerical simulations are a good candidate to investigate the fundamental mechanisms of plasma-assisted ignition. For example, the phenomenological plasma-assisted combustion model developed by Castela *et al* [10] has highlighted the key role played by the radicals created by the NRP discharges

in the turbulent flame ignition. These simulations also evidenced the flow recirculation induced by the discharge which strongly impact the probability of ignition success [11]. While these simulations gave a first understanding of plasma-assisted ignition, the mechanisms of turbulent flame ignition by a series of NRP discharge remains unknown.

The objectives of the present work are to understand, through numerical investigations, the mechanisms of turbulent premixed flame ignition by a series of NRP discharges. Simulations of a bluff-body premixed turbulent burner, designed and experimented at EM2C laboratory, are performed for that purpose. The numerical strategy relies on the implementation of the recently developed plasma combustion model [10] in an Large Eddy Simulations (LES) flow solver. The modeling approach is described in Sec. 2, whereas the configuration is detailed in Sec. 3 and results are presented in Sec. 4. Finally, a scenario of plasma assisted ignition mechanism supported by a low-order model is proposed in Sec. 5.

2. Modeling plasma-assisted turbulent combustion

2.1. Nanoseconds pulsed discharges model

NRP discharges are characterized by high voltage pulses (5 to 20 kV) that last few nanoseconds and are repeated at frequencies of the order of tens of kHz. Each NRP pulse causes an increase of the electrons kinetic energy, which is transferred to the surrounding heavy particles through collisional processes. 0D modeling studies [12, 13] on the influence of the atomic particles (O, H, N) and excited species ($O_2(a^1\Delta_g)$, $H_2(v)$, $N_2(A,B,C,a^{'})$, ...), produced by nanosecond discharges, identified new kinetic pathways in the

combustion process. 1-D and 2-D simulations of lean laminar flame ignition by NRP discharges [14–16] showed a discharge chemical effects on the combustion with an important production of radicals such as O, OH, H, CH_3 that causes a kinetic enhancement and a thermal effect that leads to a thermal enhancement. These numerical methods aims to solve the governing equations for the electric field and the electron energy, as well as the continuity equations for neutral and excited species, and the energy, mass and momentum balance equations for the gas mixture. Despite their accuracy, these strategies require high computational resources which are too expensive for 3-D turbulent flame simulations.

A semi-empirical model has been proposed by Castela *et al.* [10] to capture the effects of the NRP discharge on combustion without solving the electric field and the detailed plasma chemistry. The model considers that the NRP discharges induces mainly an electronic and vibrational excitation of nitrogen molecules as observed in [17]. The nano-second scale relaxation of nitrogen electronic states leads to an ultra-fast increase of gas temperature and dioxygen dissociation into atomic oxygen [5], whereas the relaxation of the vibrational states causes a a slow gas heating at the milliseconds scale. Ultra-fast and slow processes are modeled by spliting the rate of energy $\dot{E}^p$ deposited at each pulse in the reactive mixture into three contributions:

$$\dot{E}^p = \dot{E}^p_{chem} + \dot{E}^p_{heat} + \dot{E}^p_{vib} \tag{1}$$

The chemical $\dot{E}^p_{chem}$ and thermal $\dot{E}^p_{heat}$ terms refer to the amount of energy transferred into the ultra-fast dissociation of O_2 molecules and gas heating, respectively. The rate of energy $\dot{E}^p_{vib}$ contributes to the vibrational excitation

of N_2. According to [10], these energy contributions are modeled as follow:

$$\dot{E}^p_{chem} = \eta \, \frac{Y_{O_2}}{Y^f_{O_2}} \, (1 - \frac{e_{O_2}}{e_O}) \, \dot{E}^p \tag{2}$$

$$\dot{E}^p_{heat} = [\alpha - \eta \, \frac{Y_{O_2}}{Y^f_{O_2}} \, (1 - \frac{e_{O_2}}{e_O})] \, \dot{E}^p \tag{3}$$

$$\dot{E}_{vib} = (1 - \alpha) \, \dot{E}^p \tag{4}$$

where $Y^f_{O_2}$ represents the mass fraction of O_2 in the fresh mixture prior to each pulse. e_k is the internal energy of species in mass units. α is the ratio of energy deposited at the ultra-fast time scale, whereas η is the amount of O_2 dissociated into O atoms. These parameters are here set to $\alpha = 55\%$ and $\eta = 35\%$, according to experimental [5] and numerical [18] studies of the NRP discharge properties. The ability of the NRPD model to reproduce the discharge effects (O_2 dissociation, ultra-fast and slow heating) has been validated against measurements in [10].

2.2. LES balance equations

The plasma-combustion is coupled with the LES reactive flow governing equations combined with the Thickened Flame model for TFLES [19]. It consists in artificially thickening the reaction zone to enable the proper resolution of the flame front on a practical LES grid. In addition to the mass and momentum equations, the following balance equations are solved for total energy e, vibrational energy e_{vib} and species mass fractions Y_k:

$$\frac{\partial \overline{\rho}\widetilde{e}}{\partial t} + \frac{\partial (\overline{\rho}\widetilde{u_i}\widetilde{e})}{\partial x_i} = \frac{\partial}{\partial x_i}\left(C_p \left[F\Xi \frac{\mu}{P_r} + (1-S)\frac{\mu_t}{P_r^t} \right] \frac{\partial \widetilde{T}}{\partial x_i} \right) + \frac{\partial}{\partial x_i}\left(\sum_{k=1}^{N} \left[F\Xi \frac{\mu}{S_{c,k}} + (1-S)\frac{\mu_t}{S_{c,k}^t} \right] \frac{\partial \widetilde{Y_k}}{\partial x_i} \widetilde{h}_{s,k} \right) + \frac{\partial (\overline{\sigma_{ij} u_i})}{\partial x_i} + \overline{\dot{E}}_{chem}^{p} + \overline{\dot{E}}_{heat}^{p} + \overline{\dot{R}}_{VT}^{p} \tag{5}$$

$$\frac{\partial \overline{\rho}\widetilde{e}_{vib}}{\partial t} + \frac{\partial (\overline{\rho}\widetilde{u_i}\widetilde{e}_{vib})}{\partial x_i} = \frac{\partial}{\partial x_i}\left(\left[\frac{\overline{\mu}}{S_{c,evib}} + \frac{\mu_t}{S_{c,evib}^t} \right] \frac{\partial \widetilde{e}_{vib}}{\partial x_i} \right) + \overline{\dot{E}}_{vib}^{p} - \overline{\dot{R}}_{VT}^{p} \tag{6}$$

$$\frac{\partial \overline{\rho}\widetilde{Y_k}}{\partial t} + \frac{\partial (\overline{\rho}\widetilde{u_i}\widetilde{Y_k})}{\partial x_i} = \frac{\partial}{\partial x_i}\left(\left[F\Xi \frac{\overline{\mu}}{S_{c,k}} + (1-S)\frac{\mu_t}{S_{c,k}^t} \right] \frac{\partial \widetilde{Y_k}}{\partial x_i} \right) + \frac{\Xi}{F} W_k \overline{\dot{\omega}}_k^c + W_k \overline{\dot{\omega}}_k^p \tag{7}$$

where $\overline{\varphi}$ and $\widetilde{\varphi}$ are Reynolds and Favre filtering of variable φ. μ, S_c and P_r are the viscosity, the Schmidt and Prandtl numbers, respectively, where t superscript denotes for turbulent quantities. The dynamical formulation of the thickening factor reads $F = 1 + (F_{\max} - 1)S$, where the flame sensor S equals 0 and 1 outside an inside the reactive layer, respectively. Ξ is the subgrid scale flame wrinkling. $\overline{\dot{\omega}}_k^c$, the chemical reaction rate due to combustion, is modeled by a detailed mechanism.

The plasma chemical reaction rate $\overline{\dot{\omega}}_k^p$ is closed to account for the O_2 dissociation induced by the electrical discharge:

$$\overline{\dot{\omega}}_O^p = \eta \, \frac{\widetilde{Y}_{O_2}}{Y_{O_2}^f} \, \frac{\dot{E}^p}{e_O \, W_O} \tag{8}$$

$$\overline{\dot{\omega}}_{O2}^p = -\frac{W_O}{W_{O2}} \, \overline{\dot{\omega}}_O^p \tag{9}$$

$$\overline{\dot{\omega}}_k^p = 0 \quad \text{if k} \neq O_2,\, O \tag{10}$$

As the plasma chemistry is much faster than flow mixing, sub-grid scale interactions between turbulence and plasma chemistry have been neglected. The term $\dot{R}_{VT}^p$ in both Eq. (5) and Eq. (6) refers to the relaxation rate of the vibrational energy into gas heating. It is modelled considering the Landau-Teller harmonic oscillator approach [20]:

$$\overline{\dot{R}}_{VT}^p = \overline{\rho}\ \frac{\widetilde{e}_{vib} - e_{vib}^{eq}(\widetilde{T})}{\tau_{VT}} \tag{11}$$

where the equilibrium value of the vibrational energy, $e_{vib}^{eq}(T)$, at a given gas temperature T, is given by $e_{vib}^{eq}(T) = r\ \Theta_1/(\exp(\Theta_1/T) - 1)$, with $\Theta_1 = 3396K$ and $r = R/W_{N_2}$, R being the gas constant and W_{N_2} the molar mass of nitrogen. τ_{VT} is computed according to [10]. The filtered rate of energy, $\overline{\dot{E}}_{chem}^p$,$\overline{\dot{E}}_{heat}^p$ and $\overline{\dot{E}}_{vib}^p$ are closed from Eq. (2), Eq. (3) and Eq. (4) by neglecting sub-grid scale contribution, i.e. by assuming that $\overline{\dot{E}_y^p} = \dot{E}_y^p(\widetilde{Y}_{O_2}, \overline{\dot{E}}^p)$.

3. MiniPAC configuration

3.1. Experimental set up

The MiniPAC configuration, sketched in Fig.1(a), is a premixed methane-air bluff-body stabilized turbulent flame. The injection tube and the bluff-body diameters are $D_i = 1.6$ cm and $D_b = 1$ cm, respectively. The burner is fed with a methane-air mixture ($\phi = 0.95$), injected at a constant mass flow rate $\dot{m} = 15\ m^3\ h^{-1}$ which corresponds to a bulk velocity $U_b = 37.5$ m.s^{-1}. 10 kV discharges, corresponding to a reduced electric field (E/N) of 100 Td to 300 Td (1Td = 10^{-21}V.m^2) are applied using a 2 mm diameter electrode positioned 5 mm above the bluff body and connected to a high frequency

pulse generator. The images of the discharge during the pulses show that the discharge has a quasi-cylindrical shape of 5 mm length corresponding to the inter-electrode distance, and a radius equal to 1.75 mm. Electrical measurements of the voltage and the current showed that each discharge pulse transfers 3.5 mJ to the flow. The deposit lasts 50 ns and is repeated at a frequency of 20 kHz.

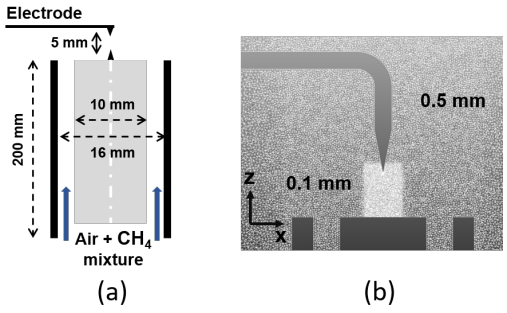

Figure 1: (a) MiniPAC burner scheme. (b) mesh in the near-electrode region

3.2. Numerical set up

LES of the MiniPAC burner ignition sequence are performed using the YALES2 unstructured finite-volume low-Mach number solver [21]. The time integration is performed using a fourth-order temporal scheme with a centred fourth order scheme for spatial discretization. The sub-grid Reynolds stresses tensor is closed using the Dynamic Smagorinsky model [22]. The COFFEE kinetic scheme involving 14 species and 38 reactions is used for the methane-air mixture chemistry [23], species equations are coupled with turbulence using the Thickened Flame model for LES (TFLES) [19] and the Charlette sub-grid scale flame wrinkling model [24].

The discharges properties have been set to be consistent with experimental measurements for the temperature and the atomic oxygen spatial

distribution and the deposited energy. The discharge has a cylindrical shape filtered with the spatial function $F(r) = erfc[(r/a)^b]$ where r is the radial distance from the discharge axis. a and b are geometric parameters, fitted to model the measured discharge radius and to ensure a sufficient numerical resolution of the discharge interface.

A fraction of the energy deposited by the discharge leaves the domain in the form of acoustic waves causing locally a temperature decay [10]. Since the low-Mach number formulation can not capture acoustic waves, the amount of acoustic discharge energy leaving the domain has been evaluated from the DNS computations [10] and then deducted from the amount of energy deposited in the low-Mach LES solver [21].

The computational domain includes half of the injection tube and covers 35 D_b and 30 D_b in downstream and radial directions, respectively. To identify the optimal spatial resolution of the the plasma, a series of five electrical pulses has been computed on three different grids characterized by cells sizes of 25 μm, 50 μm, and 100 μm in the discharge zone. Figure. 2 shows that the evolution of the maximum temperature and O concentration in the discharge zone is similar on each grid, even on the coarser mesh 100 μm which is therefore retained to conduct the LES. As the discharge interface is well resolved by this grid, no influence of TFLES model is expected in this region. The final mesh therefore consists of 40 millions of tetrahedral elements. In the plasma discharge zone the cells size equals 0.1 mm while in the flame zone it ranges from 0.1 mm to 0.5 mm. A 2-D view of the mesh in (x,z) plane is illustrated in Fig. 1(b) in the near-electrode region.

Two different simulations, indicated as cases LES-T and LES-TC in

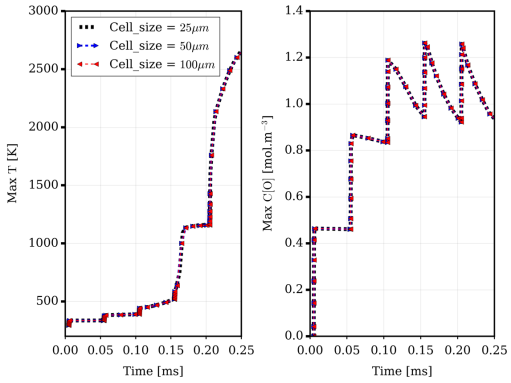

Figure 2: Sensitivity study of the grid resolution in the discharge zone. Temporal evolution of maximal values of temperature and atomic oxygen O concentration reached in the discharge are plotted during 5 pulses. Three different mesh size are tested, corresponding to cell size of 25 μm (black), 50μm (blue) and 100 μm (red, retained for the LES) in the discharge zone.

Tab. 1, are performed to understand the role of species dissociation in the turbulent flame ignition mechanism. In both simulations, 55% of the energy is deposited at the ultra-fast scale ($\alpha = 0.55$) whereas 45% is transferred into the vibrational energy, which relax slowly into gas heating. In LES-T case, only thermal effects are considered in the plasma discharge model ($\eta = 0$). In LES-TC case, in accordance with experimental and numerical observations [5, 18] 35 % of O_2 is dissociated into O atoms during the pulse. For both cases, the same amount of energy of 3.5 mJ per pulse is transferred to the flow.

4. Results

For both cases, the NRP discharges are applied at time $t = 0$ with a pulse frequency of 20 kHz. Figure 3 shows a series of 2-D instantaneous snapshots in the plane (y,z) of the temperature field for case LES-T, where only thermal

Case	α	η	Discharge properties
LES-T	0.55	0.0	heating
LES-TC	0.55	0.35	heating and O_2 dissociation

Table 1: Numerical case properties. The same amount of energy per pulse E_p=3.5 mJ is deposited for each case.

effects of the plasma are considered. The temperature in the discharge zone increases after each pulse until it reaches a steady state after approximately 15 pulses. The heat brought by the discharge diffuses in the recirculation zone located downstream the bluff body but the mixture does not ignite. Although the pulse generator is always turned on, no flame kernel is formed. Figure 4 shows instantaneous fields of temperature for LES-TC solution, where both thermal and chemical properties of the plasma are considered. A reactive kernel is now clearly identified after only 5 pulses at $t = 200\ \mu s$, leading to local ignition. Even if the pulse generator is turned off after the 10^{th} discharges, the kernel still growths and transits to a turbulent V shaped flame, which reach a steady-state regime at $t = 7.5$ ms.

These observations are confirmed by the temporal evolution of computational domain maximum temperature, plotted in Fig. 5. When only thermal effects are considered, the temperature never reaches the burnt gases temperature level, despite the unceasing plasma pulsations. Indeed, despite two peaks at 2000 K observed at $t = 0.75$ ms and $t = 2.75$ ms, the maximal temperature fluctuates around 1200 K. At the opposite, when both chemical and thermal plasma effects are considered, ignition is clearly identified after the 5^{th} pulse. A peak above 4000 K is then reached at the center of the discharge.

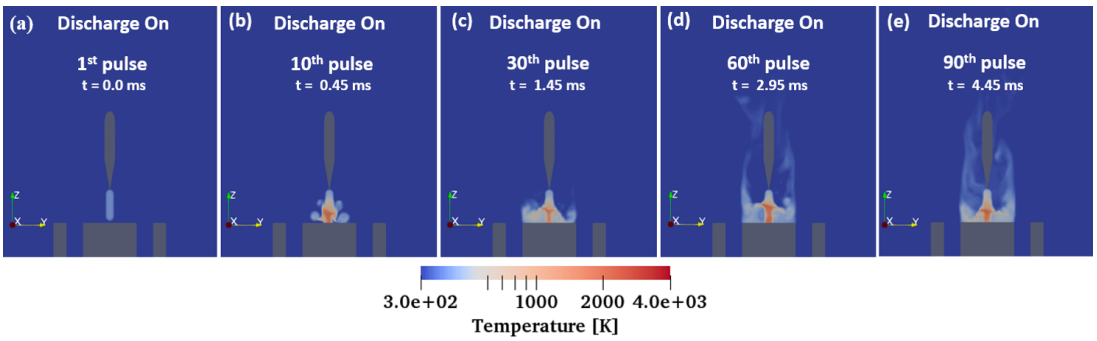

Figure 3: Simulation of the ignition attempt of the MiniPAC configuration by a series of NRP discharges, case LES-T, Only the thermal effects are taken in account ($\eta = 0$). Instantaneous 2-D temperature fields are shown at the: 1^{st} (a), 10^{th} (b), 30^{th} (c), 60^{th} (d), 90^{th} (e) plasma pulses. Ignition never occur even after 90 pulses.

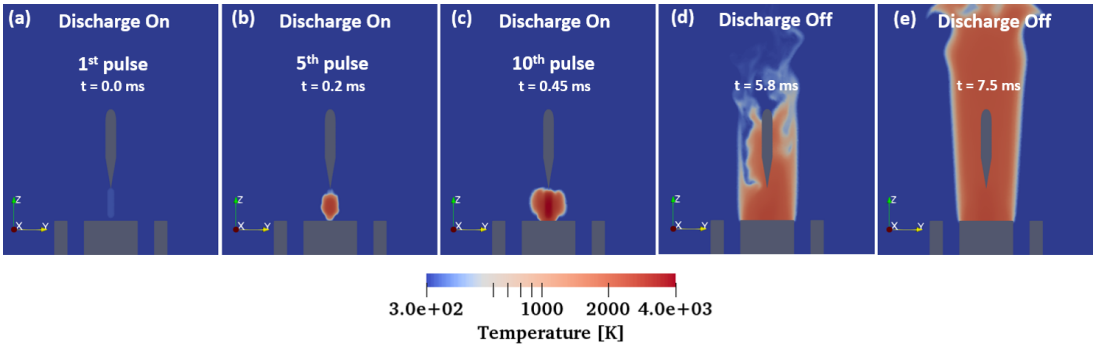

Figure 4: Simulation of the ignition attempt of the MiniPAC configuration by a series of NRP discharges, case LES-TC, both the thermal and the chemical effects are taken in account ($\eta = 0.35$). Instantaneous 2-D temperature fields are shown at the: 1^{st} (a), 5^{th} (b), 10^{th} (c) plasma pulse and at t = 5.8 ms (d) and t = 7.5 ms when the pulses generator is off. The flame ignites at the 5^{th} pulse (b) and transits to form a V flame in (d) and (e).

The combustion is even sustained when the NRP discharges are turned off after the 10^{th} pulse. Figure. 6 shows the temporal evolution of the maximal O concentration computed in the LES. The LES-TC case exhibits a signifi-

cant production of atomic oxygen O by the discharge whose concentrations reach 1.2 $mol.m^{-}3$ just before ignition. When the discharge is turned off, atomic oxygen O concentration decreases to equilibrium conditions. Situation is very different in LES-T case, where the oxygen concentration remains equal to zero and no ignition is observed.

These results are qualitatively consistent with undergoing experiments campaigns conducted at EM2C laboratory, where flame ignition is always successful after a series of NRP discharges. Unfortunately, the exact number of discharges required to ignite the flame is not known, preventing quantitative validation of the simulations against experimental measurements. However, to further understand the mechanism of turbulent flame ignition by the plasma, an analysis based on a Perfectly Stirred Reactor (PSR) analogy is proposed in the following section.

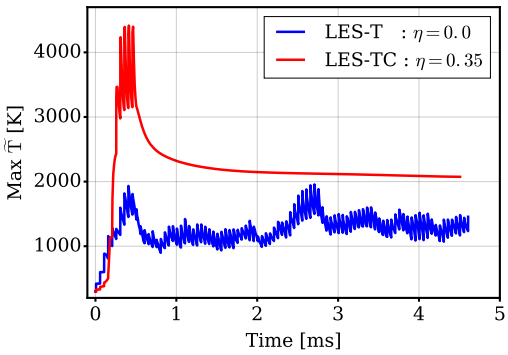

Figure 5: Temporal evolution of the maximum value of gas temperature in the MiniPAC simulations. The mixture ignites after 5 pulses for case LES-TC (red), whereas ignition never occurs for case LES-T (blue).

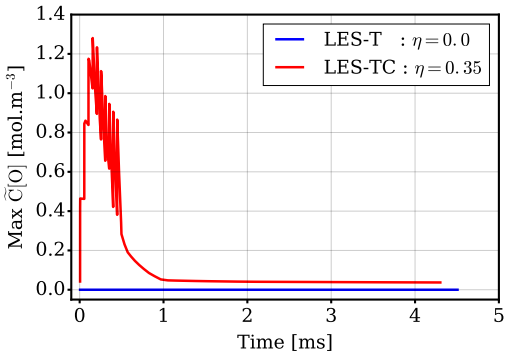

Figure 6: Temporal evolution of the maximum atomic oxygen O concentration in the MiniPAC simulations, LES-TC (red), LES-T (blue)

.

5. Scenario of ignition mechanism by NRP discharge

The NRP energy deposition causes an ultra-fast increase of the gas temperature, which generates a gas expansion. It creates two recirculation zones, promoting fresh gas entrainment into the discharge channel [11]. This phenomena is evidenced in Fig. 7(a), which shows the velocity stream-lines superimposed on the temperature field in the inter-electrode region, at $t = 25\ \mu s$ after a pulse discharge. Ignition success or failure results from competition between the residence time of the reacting gases in the discharge zone and the combustion chemistry time scale. This phenomena is modeled by a PSR schematized in Fig. 7(b), whose volume matches the discharge channel of diameter d. The flow of gas passing through the PSR reproduces the recirculating gases at velocity V.

Residence time of the mixture in the PSR is therefore given by $\tau = d/V$. The PSR balance equations reads:

$$\frac{dh}{dt} = \frac{1}{\tau}\left(\sum_{k=1}^{K} Y_{k0}h_{k0} - \sum_{k=1}^{K} Y_k h_k\right) - \frac{Q_h}{\rho V} + \dot{E}^p_{chem} + \dot{E}^p_{heat} + \dot{R}^p_{VT} \tag{12}$$

$$\frac{dY_k}{dt} = \frac{1}{\tau}\left(Y_{k0} - Y_k\right) + \frac{W_k\dot{\omega}^c_k}{\rho} + \frac{W_k\dot{\omega}^p_k}{\rho} \tag{13}$$

$$\frac{de_{vib}}{dt} = \frac{1}{\tau}\left(e_{vib0} - e_{vib}\right) + \dot{E}^p_{vib} - \dot{R}^p_{VT} \tag{14}$$

where 0 subscript denotes fresh gases properties flowing in the PSR. The rate of deposited thermal and chemical energies $\dot{E}^p_{chem}$, $\dot{E}^p_{heat}$ and $\dot{E}^p_{vib}$ are closed according to Eq. (2), Eq. (3) and Eq. (4). The relaxation rate of vibrational energy $\dot{R}^p_{VT}$ is modeled by Eq. (11) and the plasma chemistry sources terms $\dot{\omega}^p_k$ is closed by Eq. (8), Eq. (9) and Eq. (10).

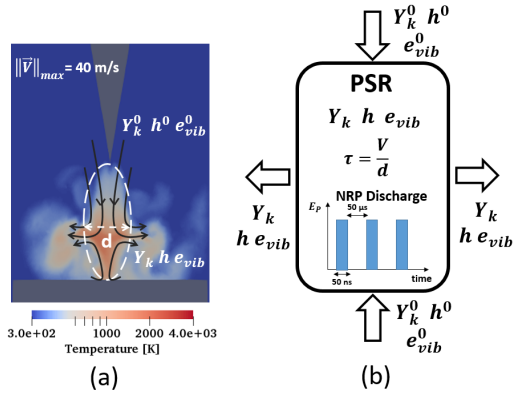

Figure 7: (a) flow recirculation in the discharge channel after a pulse. (b) PSR modeling of plasma-assisted ignition mechanism.

PSR-T refers to simulations conducted by considering only thermal effects, whereas PSR-TC computations accounts for chemical plasma properties. Examples of PSR-T and PSR-TC solutions are plotted in Fig.8 for

$\phi = 0.95$ at a residence time $\tau = 3.10^{-4}$ s, with the same discharge properties as those used in Sec. 3. PSR-T simulation requires 12 pulses to ignite the mixture whereas only 6 pulses are needed by PSR-TC. In accordance with [10], for the same amount of deposited energy, the chemical effect of O radical is more important than the temperature on the ignition process. Due to its high reactivity, the atomic oxygen O enhances the hydrocarbon oxidation reactions even at low gas temperatures, which reduces the combustion chemistry time scale and therefore the ignition delays.

PSR results are used to established a plasma-assisted ignition diagram. For each PSR simulation, the pulse generator is maintained until 80% of the fuel mass fraction is consumed. Following this criteria, the minimal number of pulses required to form a flame kernel is plotted in term of the recirculation zone residence time in Fig. 9. Blue and red symbols correspond to PSR-T and PSR-TC solutions, respectively. Production of atomic oxygen significantly reduces the number of pulses needed for ignition. Difference between PSR-T and PSR-TC is even more pronounced when the residence times decreases. The critical residence below which ignition never occurs equals 0.15 ms for pure thermal discharges, whereas it decreases to 0.08 ms when chemical effects are accounted for.

Practical residence times are estimated from the maximal velocity reached within the recirculation vortices induced by the discharge. By this way, two residence times 0.05 ms $< \tau_T <$ 0.08 ms and 0.2 ms $< \tau_{TC} <$ 0.3 ms are estimated from LES-T and LES-TC solutions, respectively. Note that a higher amount of heat is deposited in LES-T, the gas expansion is more important and the velocity is larger than in LES-TC. It explains why $\tau_T <$

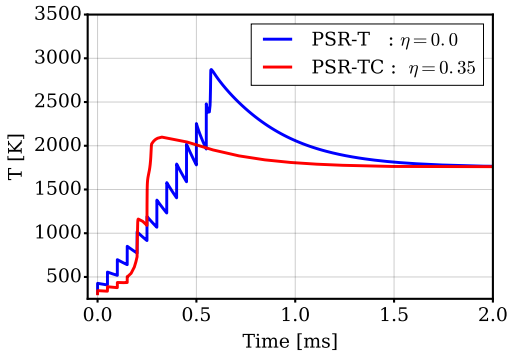

Figure 8: temperature temporal evolution for both PSR-T (blue) and PSR-TC (red) simulations for $\tau = 0.3$ ms. For PSR-TC case, ignition occurs after 6 pulses, whereas for PSR-T case, ignition occurs after 12 pulses.

τ_{TC} . Residence times τ_T and τ_{TC} encountered in the LES are indicated in Fig. 9 by red and blue area. According to the PSR-TC diagram, the flame should ignite after 6-7 pulses. This is consistent with LES-TC simulations where ignition occurs between 5 and 10 pulses. The blue area is however located outside the ignition conditions whatever the number of discharges, which is consistent with the ignition failure observation in LES-T.

6. Conclusion

This article presents the first LES of turbulent flame ignition by a series of NRP discharges. The numerical investigations have been conducted with the massively parallel YALES2 solver in which a phenomenological plasma-assisted combustion model has been implemented. The retained configuration is a premixed bluff-body turbulent flame where successful ignition by NRP discharges has been experimentally observed at EM2C.

Ignition is also observed in the simulation but only if the ultra-fast dis-

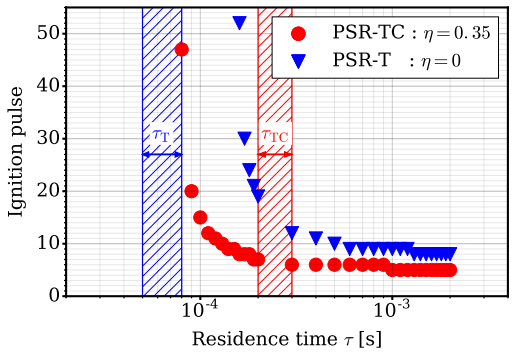

Figure 9: plasma-assisted ignition diagram. The number of pulses required to form a flame kernel in terms of the residence time. Blue symbols correspond to the PSR-T case. Red symbols correspond to the PSR-TC case. Residence times τ_T for the LES-T case and τ_{TC} for the LES-TC case are indicated by the red and the blue hatched area, respectively.

sociation of species O_2 into O induced by the NRP discharge is accounted for. LES data post-processing shows that the flow recirculation induced by the energy deposition promotes fresh gases entrainment in the discharge zone and plays a crucial role in the ignition process. Analysis of simulation results suggests that ignition success or failure results from a competition between flow mixing and combustion chemical time scales. Based on this hypothesis, a plasma-assisted combustion diagram, generated from PSR calculations, gives the number of pulse required to ignite the initial turbulent flame kernel. This PSR analogy is limited to phenomenological analysis. Whereas it helps to understand the mechanism of plasma assisted combustion, too many parameters are uncertain for being predictive.

Results presented in this article confirms that the major interest of NRP discharges is the production of radical species which directly interact with the combustion chemistry mechanism. The simulations has here been per-

formed by assuming that the production of O species by the discharge is the key chemical effect of plasma on combustion chemistry. This assumption is not restrictive with respect to the modeling strategy, which will be extended in the future to account for other radicals production and possible fuel dissociation induced by the plasma discharge.

Acknowledgments

This work was supported by the ANR programs PASTEC (ANR-16-CE22-0005-01) and granted access to the HPC resources from IDRIS, TGCC and CINES under the allocation A0032B10253 and A0052B10253 made by GENCI (Grand Equipement National de Calcul Intensif) and HPC resources from the Mesocentre computing center of CentraleSupelec and Ecole Normale Superieure Paris-Saclay supported by CNRS and Rgion Ile-de-France (http:// mesocentre.centralesupelec.fr/). Vincent Moureau and Ghislain Lartigue from CORIA lab, and the SUCCESS scientific group are acknowledged for providing the YALES2 code.

References

[1] A. Starikovskiy, N. Aleksandrov, Plasma-assisted ignition and combustion, Progress in Energy and Combustion Science 39 (2013) 61-110.

[2] Y. Ju, W. Sun, Plasma assisted combustion: dynamics and chemistry, Progress in Energy and Combustion Science 48 (2015) 21-83.

[3] D. Galley, G. Pilla, D. A. Lacoste, F. Lacas, D. Venante, C. O. Laux, Plasma enhanced combustion of a lean premixed air., In 43th AIAA

Aerospace Sciences Meeting and Exhibit Reno, NV USA. AIAA (2005) 1193.

[4] G.Pilla, D. Galley, D. A. Lacoste, F. Lacas, D. Veynante, C. Laux., Stabilization of a turbulent premixed flame using a nanosecond repetitively pulsed plasma, Plasma Science, IEEE Transactions on 34 (2006) 2471-2477.

[5] D. L. Rusterholtz, D. A. Lacoste, G. D. Stancu, D. Z. Pai, C. O. Laux, Ultrafast heating and oxygen dissociation in atmospheric pressure air by nanosecond repetitively pulsed discharges., Journal of Physics D: Applied Physics 46, 464010 (2013).

[6] A. Lo, A. Cessou, P. Boubert, P. Vervisch, Space and time analysis of the nanosecond scale discharges in atmospheric pressure air: I. gas temperature and vibrational distribution function of n2 and o2, J Phys D: Appl Phys.47:115201 (2014).

[7] R. M. S. Macheret, M. Shneider, Energy efficiency of plasma assisted combustion in ram/scramjet engines, 36th AIAA Plasma dynamics and Lasers Conference, Toronto, Ontario, Canada. (2005).

[8] S. Lovascio, T. Ombrello, J. Hayashi, S. Stepanyan, D. Xu, G. Stancu, C. Laux, Effects of pulsation frequency and energy deposition on ignition using nanosecond repetitively pulsed discharges, Proceedings of the Combustion Institute 36 (2017) 4079-4086.

[9] J. Lefkowitz, T. Ombrello, An exploration of inter-pulse coupling in

nanosecond pulsed high frequency discharge ignition, Combustion and Flame 180 (2017) 136-147.

[10] M.Castela, B.Fiorina, A.Coussement, O.Gicquel, N.Darabiha, C.O.Laux, Modelling the impact of non-equilibrium discharges on reactive mixtures for simulations of plasma-assisted ignition in turbulent flows, Combustion and Flame 166 (2016) 133-147.

[11] M. Castela, B. Fiorina, S. Stepanyan, A. Coussement, O. Gicquel, N. Darabiha, C. Laux, A 3-d dns and experimental study of the effect of the recirculating flow pattern inside a reactive kernel produced by nanosecond plasma discharges in a methane-air mixture, Proceedings of the Combustion Institute 36 (2017) 4095-4103.

[12] N. A. Popov, The effect of nonequilibrium excitation on the ignition of hydrogen-oxygen mixtures., High Temperature (2007).

[13] S. Williams, S. Popovic, L. Vuskovic, C. Carter, L. Jacobson, S. Kuo, D. Bivolaru, S. Corera, M. Kahandawala, S. Sidhu, Model and igniter development for plasma assisted combustion, 42nd AIAA Aerospace Sciences Meeting and Exhibit, Reno, NV, AIAA (2004) 1012.

[14] H. Takana, H. Nishiyama, Numerical simulation of nanosecond pulsed dbd in lean methaneair mixture for typical conditions in internal engines, Plasma Sources Science and Technology 23 034001 (2014).

[15] F. Tholin, D. Lacoste, A. Bourdon, Influence of fast-heating processes and o atom production by a nanosecond spark discharge on the ignition

of a lean h2/air premixed flame, Combustion and Flame 161 (2014) 1235-1246.

[16] T. A. Casey, J. Han, M. Belhi, P. G. Arias, F. Bisetti, H. G. Im, J.-Y. Chen, Simulations of planar non-thermal plasma assisted ignition at atmospheric pressure, Proceedings of the Combustion Institute 36 (2017) 41554163.

[17] N. Popov, Investigation of the mechanism for rapid heating of nitrogen and air in gas discharges., Plasma Physics Reports 27 (10), 886-896. (p. 25, 39, 49) (2001).

[18] N. A. Popov, Fast gas heating initiated by pulsed nanosecond discharge in atmospheric pressure air., AIAA Aerospace Sciences Meeting, Grapevine, TX, 7/10 January, (2013) 105251. (p. 50).

[19] O. Colin, F. Ducros, D. Veynante, T. Poinsot, A thickened flame model for large eddy simulations of turbulent premixed combustion, Physics of Fluids 12, 1843 (2000).

[20] L. Landau, E. Teller, Zur theorie der sohdldispersion., Physik. Z. Sowjetmion, 10, 34 (1936).

[21] V. Moureau, Yales2, yales2.coria-cfd.fr (2010).

[22] M. Germano, U. Piomelli, P. Moin, W. Cabot, A dynamic subgrid-scale eddy viscosity model., Physics of Fluids A: Fluid Dynamics (1989 1993), Vol. 3, No. 7, 1991, pp. 17601765.

[23] T. COFFEE, Kinetic mechanisms for premixed, laminar, steady state methane/air flames, Combustion and Flame 55:161 170 (1984).

[24] F. Charlette, D. Veynante, C. Meneveau, A power-law wrinkling model for les of premixed turbulent combustion: Part i non dynamic formulation and initial tests., combustion and flame 131 (2002) 159–180.